# A study of precursors to equatorial spread *F* using the Giant Meterwave Radio Telescope

A. DasGupta,[1,2] A. Paul,[1] S. Ray,[2] A. Das,[2] and S. Ananthakrishnan[3]

Received 27 March 2007; revised 24 March 2008; accepted 18 July 2008; published 11 September 2008.

[1] This paper reports the results of an experiment to identify a possible precursor to equatorial spread *F* (ESF) with the Giant Meterwave Radio Telescope (GMRT) (latitude: 19.10°N, longitude: 74.05°E geographic; dip: 23°N magnetic) near Pune by simultaneously recording the amplitude and phase of the signal from the radio source 3C218 (RA:$09^h15^m$, Declination:−11°) at 235, 327, 610, and 1420 MHz in the postsunset-premidnight period 18.5–22.5 LT on 26, 29, and 31 March 2004. Patches of scintillations both in amplitude and phase were observed on 26 and 29 March 2004 at 235, 327, and 610 MHz frequencies starting around 20 LT (LT = UT + 05:00) and extending until 22 LT while the records for 31 March 2004 do not show any scintillations. Significant amplitude scintillations were not observed at 1420 MHz. The most remarkable feature was the presence of large-scale periodic structures in phase prior to onset of amplitude scintillations. The Total Electron Content (TEC) as observed on a GPS link also looking through the same ionospheric volume showed periodic variation of carrier phase prior to onset of scintillations and bite-outs in TEC, which implies that before the onset of ESF, the large-scale wave structures propagate to the height of maximum ionization and beyond.

**Citation:** DasGupta, A., A. Paul, S. Ray, A. Das, and S. Ananthakrishnan (2008), A study of precursors to equatorial spread *F* using the Giant Meterwave Radio Telescope, *Radio Sci.*, *43*, RS5002, doi:10.1029/2007RS003667.

## 1. Introduction

[2] The Earth's ionosphere acts as a perturbing medium on transionospheric radio signals coming from a radio source or a satellite. The propagation effects introduced by the ionosphere, such as, refraction leading to an angular error in the direction of arrival of the signal, differential Faraday rotation and scintillations, are most severe in the equatorial region covering ± 30° dip around the magnetic equator. The equatorial ionosphere is characterized by the equatorial ionization anomaly occurring over a major part of the day and intense ionization density irregularities, which usually generate over the magnetic equator in the postsunset hours. The morphology of the equatorial ionosphere is quite different from that at other latitudes because the magnetic field **B** is nearly parallel to the Earth's surface. During daytime, the *E* region dynamo electric field **E** is eastward. Due to the 'fountain effect', the resulting **E** × **B** drift transports ionospheric *F* region plasma upward at the magnetic equator. The uplifted plasma then moves along **B** in response to gravity and pressure-gradient forces and forms the equatorial anomaly with minimum *F* region ionization density at the magnetic equator and maxima at the two crests approximately 15° to 20° in magnetic latitude to the north and south. The equatorial ionization anomaly results in large gradients of ionization in horizontal as well as vertical directions. Near sunset, plasma densities and dynamo electric fields in the *E* region decrease, and the equatorial anomaly begins to weaken. However, at this local time, a dynamo develops in the *F* region. Polarization charges within conductivity gradients at the terminator enhance the eastward electric field after sunset. The postsunset electric field moves the ionospheric plasma upward, allowing the equatorial anomaly crests to intensify. After sunset, *F* region dynamo currents are no longer subject to the shorting effect of the conducting *E* layer to the north and south of the magnetic equator. Polarization fields are thus able to drive the *F* layer upwards. Eventually the electric field turns westward, causing plasma to drift downward. Just before the reversal at the time of sunset, the field is much enhanced [*Rishbeth*, 1971]. This is called the postsunset or the prereversal enhancement of the eastward electric

[1]Institute of Radio Physics and Electronics, University of Calcutta, Calcutta, India.
[2]S. K. Mitra Center for Research in Space Environment, University of Calcutta, Calcutta, India.
[3]Department of Electronic Science, University of Pune, Pune, India.


0048-6604/08/2007RS003667

field. The prereversal enhancement holds the key to the formation of irregularities. Irregularities develop in the evening at *F* region altitudes of the ionosphere in the form of depletions, frequently referred to as 'bubbles'. The depletions originate over the magnetic equator in the postsunset hours and extend in both horizontal and vertical directions. The bubbles are upwelled by electrodynamic $\mathbf{E} \times \mathbf{B}$ drift over the magnetic equator and map down to off-equatorial locations along magnetic field lines. As the bubbles move, normally from west-to-east across a satellite link, ionization depletions and scintillations are encountered.

[3] Excellent review articles on equatorial ionospheric *F* region irregularities are available [*Fejer and Kelley*, 1980]. Scattering of signals from these irregularities embedded in the ionosphere are obtained in the form of spread *F* on radar maps [*Woodman and La Hoz*, 1976; *Fejer and Kelley*, 1980]. Plasma depletions were first observed by the polar orbiting OGO-6 satellite [*Hanson and Sanatani*, 1973]. The irregularities, in the form of depletions, manifest as deep bite-outs in in situ density plots [*Kelley et al.*, 1976; *McClure et al.*, 1977], and cause scintillations in transionospheric satellite links [*Basu and Basu*, 1976; *Basu and Whitney*, 1983]. *Kil and Heelis* [1998a] have reported the global distribution of ionospheric irregularities from the Atmospheric Explorer-E (AE-E) satellite data. Airglow observations with all-sky cameras establish that the irregularity clouds become narrower with latitude on both sides of the magnetic equator [*Weber et al.*, 1980]. Both airglow observations and scintillations with orbiting satellites show that the irregularity clouds may split into several streams as one moves away from the equator [*Bhar et al.*, 1970].

[4] The development of equatorial spread *F* (ESF) extending from the bottomside to the topside of the equatorial ionosphere leads to generation of irregularities with scale sizes extending over six orders of magnitude from centimeter to hundreds of kilometer ranges through cascading plasma processes. The most spectacular effect observed on transionospheric VHF/UHF radio waves is that of scintillations of amplitude and phase of the signal. Amplitude scintillation is effectively produced by irregularities of first Fresnel dimension scale size [*Rufenach*, 1972, 1975; *Basu and Whitney*, 1983] i.e., VHF amplitude scintillations of satellite and radio source signals correspond to irregularities of kilometer scales whereas the microwave signals are affected by decameter/hectometer scales. The sparse phase scintillation measurements however cover an extended part of the spectrum. It is advisable that a combination of amplitude and phase scintillations may provide vital information about the spectrum.

[5] For the generation of irregularities, a certain perturbation in the bottomside of the *F* layer is necessary. The seed mechanism for these perturbations is not yet fully understood. Gravity waves have been suggested to be one of the candidates [*Kelley et al.*, 1981, 1986; *Hysell et al.*, 1990]. There are indications that at times of daytime scintillations also, the vertical distribution of ionization in the sporadic *E* layer may be influenced by short period gravity waves [*DasGupta and Kersley*, 1976]. Although the fundamental necessity for a plasma instability process is now well established, this does not rule out an important role for the dynamics of the neutral atmosphere in controlling or modifying the phenomenon. *Rottger* [1973, 1976, 1978] presented strong evidence for the organization of *F* layer ionization into large-scale wavelike ionization structures and argued that gravity wave mechanism might be responsible. *Klostermeyer* [1978] made a nonlinear calculation of the effect of spatial resonance and concluded that gravity waves could indeed organize the *F* layer plasma into large-scale horizontally modulated contours. Furthermore, the Rayleigh-Taylor growth rate is small ($\sim 10^{-4} s^{-1}$), and growth from ion density variations due to thermal fluctuations may not be quick enough to account for the rapid development after sunset.

[6] It is well known that a strong shear exists in the bottomside equatorial *F* region ionosphere around twilight, where the plasma flow in the bottomside reverses from westward to eastward with increasing altitude [*Kudeki et al.*, 1981; *Tsunoda et al.*, 1981]. A number of factors are thought to contribute to shear flow, including *E* region dynamo winds, vertical winds and horizontal electric fields on flux tubes with significant Hall conductivity, and vertical currents sourced in the electrojet region near the solar terminator. Which of these factors is most important remains unknown, in part because they are difficult to measure directly using in situ or remote sensing. The connection between bottomside shear and equatorial spread *F* has been investigated before, but mainly from the point of view of shear stabilization of otherwise growing waves. A series of nonlocal boundary value analyses by *Guzdar et al.* [1982] and *Huba and Lee* [1983] pointed to the stabilization of interchange instabilities by shear flow and the movement of the most unstable modes to longer wavelengths. The issue of shear flow stabilization remains unresolved, and a number of recent theoretical and computational studies continue to support the premise [*Hassam*, 1992; *Sekar and Kelley*, 1998]. *Hysell and Kudeki* [2004] have shown that fast growing waves associated with a collisional branch of the instability exist for appropriately chosen velocity, density, and collision frequency profiles, including profiles broadly representative of the equatorial *F* region.

[7] Occurrence of spread *F* is more or less a daily phenomenon in the equatorial and low-latitudes during the equinoctial months of high sunspot number years.

However, no prediction is available for occurrence of ESF on any particular evening. Recent efforts have been directed toward prediction of the day-to-day variability in terms of the seed mechanism or precursors. This prediction service has become very important in view of the deleterious effect of ESF on modern space-based communication and navigation systems. A very important component of the International Space Weather program is concerned with the development of forecasting and nowcasting techniques for equatorial ionospheric irregularities.

[8] The Giant Meterwave Radio Telescope (GMRT) (lat: 19.10°N, long: 74.05°E geographic; dip: 23°N magnetic) near Pune is located within the equatorial region of the Earth's ionosphere. It is operated by the Tata Institute of Fundamental Research (TIFR) at Khodad near Narayangaon, 80 km north of Pune and 200 km east of Mumbai. GMRT consists of 30 parabolic dish antennas of 45 m diameter arranged in a Y-shaped array. Fourteen antennas are placed in the central array, about 1 $km^2$ in size. Five antennas lie along each of the 14 km long east and south arms while six lie along the west arm. The operating frequencies of GMRT are 235, 327, 610, and 1420 MHz. A detailed description of the GMRT system could be obtained from *Swarup et al.* [1991].

[9] The Indian subcontinent essentially covers the equatorial zone in the South Asian longitudes, with the magnetic equator touching the southern tip of the peninsula near Trivandrum. A location like GMRT situated in between the magnetic equator and the northern crest of the equatorial ionization anomaly is ideally suited for studying the equatorial ionospheric irregularities. Very intense (frequently saturated) and fast scintillations of amplitude and phase of a radio signal are observed in this region of the globe in the postsunset to midnight local time sector around the equinoxes of high sunspot number years. An observational campaign at multiple frequencies, namely, 235, 327, 610, and 1420 MHz was undertaken from GMRT by the Satellite Beacon Group of the University of Calcutta on some days of the equinoctial month of March 2004. The major objective was to look for some large-scale wave-like precursors of ionospheric scintillations in the recorded signal. Since the phase scintillation power spectra cover a much more extended frequency range compared to amplitude scintillations, large-scale wave induced precursors of equatorial spread *F*, if present, could be found on the phase of the GMRT interferometric signal rather than the amplitude. Presence of any large-scale ionization structures in the recorded interferometric signals would be extremely useful to plan observational periods and look angles in advance for the radio astronomical facility. This information could be utilized in optimizing the observational capabilities of GMRT and save valuable resources including 'telescope time'.

[10] It has not been possible to conduct simultaneous amplitude and phase scintillation measurements over a wide frequency spectrum because of lack of suitable sources and observational facilities extending over VHF, UHF, and microwave bands. GMRT provides a unique opportunity for such a study by simultaneously monitoring the amplitude and phase of radio sources in the frequency range from 235 MHz to 1420 MHz. From the recorded phase of a transionospheric signal, precursors of ionospheric irregularities extended in altitude and drifting across the radio link may be identified.

[11] The Total Electron Content (TEC), which gives a height-integrated picture of ionization, is mainly weighted by the maximum ionization density. The phase change suffered by a radio wave traversing the ionosphere is proportional to the integrated ionization density along the line of sight i.e., the TEC. By monitoring the TEC and the phase of the interferometric signal obtained by tracking a radio source, presence/absence of ionospheric perturbations could be noted.

[12] The present paper reports, for the first time, results of a multifrequency amplitude and phase measurement of a transionospheric signal from a radio source undertaken at a major radio astronomy facility GMRT, in conjunction with transmissions from Global Positioning System (GPS), to identify initial perturbations preceding ESF based on the phase of a transionospheric signal and TEC.

## 2. Data

[13] Amplitude and phase of signals from a radio source 3C218 (RA: $09^h15^m$, Declination: $-11°$) were recorded with a sampling interval of 108 ms ($108 \times 10^{-3}$ s) at the GMRT site (lat: 19.10°N, long: 74.05°E geographic; dip: 23°N magnetic) near Pune at 235, 327, 610, and 1420 MHz using antennas in the central array operated in the interferometric mode during 18.5–22.5 LT of 26, 29, and 31 March 2004. The amplitude data comprises of correlation coefficients of signals received in a pair of antennas operated in the interferometric mode and has a maximum value of 1.0. The phase data shows the phase difference in degrees between a pair of antenna within ±180°. The above radio source is not an extended one at the lower frequencies of operation of GMRT, namely, 235, 327, and 610 MHz and at the small baselines involved using antennas in the central square. The extent of the source assumes importance only at higher microwave frequencies like 1420 MHz and longer baselines involving the east, west and south arms of the Y-shaped array.

[14] Equatorial ionospheric irregularities normally develop over the magnetic equator in the early evening hours and map to higher latitudes along magnetic field lines. Radio astronomy observations from a station like GMRT situated in between the magnetic equator and the

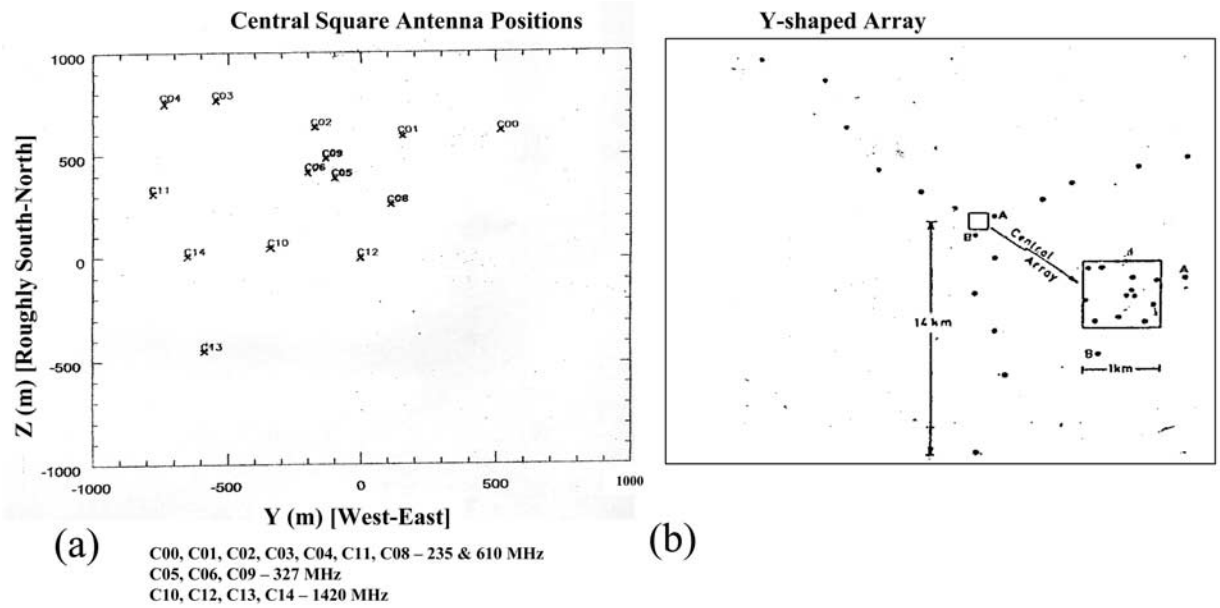


**Figure 1.** (a) Central array antenna positions at the Giant Meterwave Radio Telescope (GMRT) facility near Pune. Antennas used at different operating frequencies of GMRT for the experiment conducted are indicated. (b) Y-shaped array at GMRT.

northern crest of the equatorial anomaly in the Indian longitude sector is most likely to be affected when looking south in the postsunset hours. During the period of observation, the 350 km ionospheric pierce point of the source ranged from 17.08°–17.11°N and 76.88°–71.44°E i.e., the source moved from east to west south of the station. The 350 km subionospheric point of the radio source maps up to an apex of 500 km over the magnetic equator. The ionospheric drift velocity typically varies from about 200 m/s in the early evening hours to about 50 m/s in the postmidnight hours with an average of 100 m/s typically from west to east. The radio source transits from east to west with a velocity of 40 m/s at 350 km ionospheric height. Thus there is a relative velocity of about 140 m/s, which reduces the time difference between the event (scintillations) and precursors (periodic structures). The zonal drift precludes simultaneous observation of precursors and events, in a collocated volume in the strict sense by any single technique. However, it can be assumed that the entire region under consideration may be experiencing the same precursors. The effect of relative velocity of the source, receiver and ionosphere has been discussed by *Kintner et al.* [2004] and *DasGupta et al.* [2006] using GPS.

[15] The *F* region virtual height over the magnetic equator at Trivandrum (8.47°N, 76.91°E) rose to 409 km with a vertical upward velocity of 32 m/s on 26 March 2004 before the onset of equatorial spread *F* (ESF). On 29 March 2004, the corresponding values were 350 km and 28 m/s, respectively. On 31 March 2004 when no ESF were detected at GMRT, the *F* region virtual height over the magnetic equator attained a maximum value of 329 km with an upward velocity of 21 m/s.

[16] Antennas C00, C01, C02, C03, C04, C11, and C08 (Figure 1) were operated using dual feeds to receive both the 235 and 610 MHz signals. Antennas C05, C06, and C09 were operated at 327 MHz while C10, C12, C13, and C14 were operated at 1420 MHz. The recorded data were also subject to 16 s moving-average to remove undesired scattering of points. Scintillations were observed on the amplitude records on 26 March 2004 at 235, 327, and 610 MHz, and on 29 March 2004 at 327 and 610 MHz. Phase channels of interferometer records for 26 March 2004 showed scintillations at 235, 327, 610, and 1420 MHz while on 29 March 2004, it was observed on 327, 610, and 1420 MHz. But no such events were noted on 31 March 2004. For amplitude scintillation measurements, Automatic Level Controller (ALC) for each channel has to be disabled. Due to some problems in the operation of the ALC, the amplitude scintillation could not be recorded on some 235 and 610 MHz channels. The phase information can however be obtained even when the ALC is on.

[17] Simultaneously, under the GPS and Geo Augmented Navigation (GAGAN) program operated by the Indian Space Research Organization (ISRO), TEC on 26 March 2004 measured along several GPS links at 1 min sampling interval from Mumbai (lat: 19.09°N,

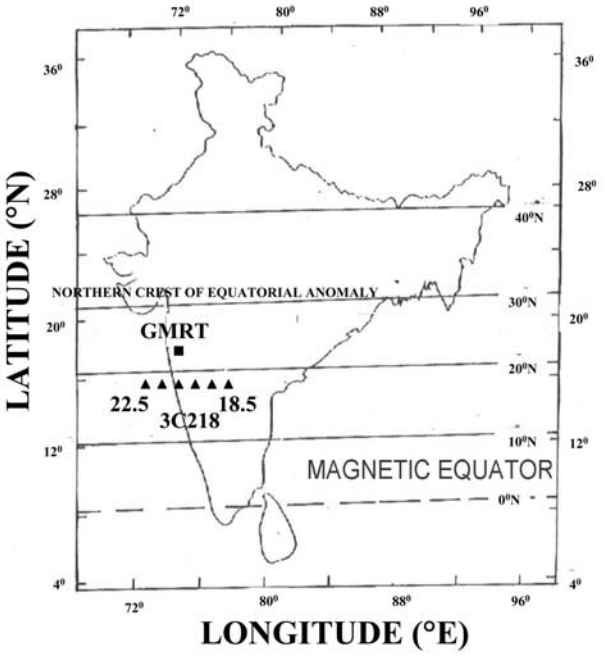


**Figure 2.** Location of GMRT site is shown on a map of India along with the 350 km ionospheric pierce point of the radio source 3C218 on 26 March 2004 during 18.5–22.5 LT. The magnetic equator and the northern crest of the equatorial ionization anomaly around 30°N dip are also shown.

long: 72.85°E geographic; dip: 25°N magnetic) were studied. The GAGAN station at Mumbai was preferred as it shared a more-or-less common ionospheric volume with GMRT observations from Pune for a number of GPS links.

## 3. Results

[18] Results of the observational campaign to identify precursors of ionospheric scintillations on the TEC and phase of a radio signal undertaken by the Satellite Beacon Group of the University of Calcutta at GMRT during the equinoctial month of March 2004 using multiple antennas at multiple frequencies ranging from VHF through UHF and L-band are presented in this section.

[19] Figure 1a shows the GMRT central square antenna positions. There are 14 antennas in the central square, namely, C00, C01, C02, C03, C04, C05, C06, C08, C09, C10, C11, C12, C13, and C14. The entire Y-shaped array is shown in Figure 1b. Out of the 14 antennas in the central square, 7 have been used at 235 and 610 MHz, 3 at 327 MHz, and 4 at 1420 MHz. An idea about the separation between the different antennas located in the central square which have been used in interferometric mode could be obtained from Figure 1a which shows the distances in meters along its two axes.

[20] Figure 2 shows the position of GMRT (19.10°N, 74.05°E geographic; dip: 23°N magnetic) and the 350 km subionospheric track of the radio source 3C218 during 18.5–22.5 LT of 26 March 2004 on a map of India. The magnetic equator and the northern crest of the equatorial anomaly around 30°N dip are also indicated. On that night, 3C218 moved from a location (17.08°N, 76.88°E) at 18.5 LT to (17.11°N, 71.44°E) at 22.5 LT i.e., more-or-less in east to west direction south of the station.

[21] Amplitude and phase of the interferometric signal from the radio source 3C218 were recorded on 26, 29, and 31 March 2004 at 235, 327, 610, and 1420 MHz at a sampling interval of 108 ms. Patches of scintillations were recorded both on the amplitude and phase channels on 26 and 29 March 2004 while the record for 31 March 2004 does not show any scintillations. The recorded data for each frequency, each antenna pair and for each date are plotted in panels, each of 1.5 h duration from left to right.

[22] On 26 March 2004, patches of scintillations were observed in the amplitudes of the interferometric signal recorded in the antenna combinations C01-C04 at 235 MHz, C09-C05, C06-C05 at 327 MHz, and C01-C04 at 610 MHz, and in the phases corresponding to the antenna combinations C01-C04 at 235 MHz, C09-C05 and C06-C05 at 327 MHz, C01-C04, C03-C00, C02-C04, C02-C03, C02-C00, C00-C01, C03-C04, C11-C02, C11-C03 at 610 MHz, and C12-C10 at 1420 MHz. However, the amplitude scintillations at 1420 MHz in the C12-C10 antenna combination were negligible.

[23] On 29 March 2004, scintillations were observed in the amplitudes corresponding to antenna combinations C06-C05, C09-C05, C09-C06 at 327 MHz and C02-C01 at 610 MHz and in the phases of C06-C05 at 327 MHz, C02-C01, C02-C03, C02-C04, C03-C04, C08-C04, C11-C02, C11-C03 at 610 MHz, and C14-C10 at 1420 MHz. Out of the total possible ${}^{n}C_{2}$ number of antenna combinations, n being the number of antennas used at a particular frequency, some antenna combinations, which showed prominent patches of scintillations, have been highlighted in the present paper. The correlation distance of scintillation causing irregularities in relation to the baseline is very important in interferometric observations. The irregularities have a power law spectrum over the scale length of range few tens of meters to tens of kilometers. The power spectral density of amplitude scintillations attain its maximum value corresponding to the scale length of $(2 \times \text{radio wavelength} \times \text{height of the irregularity layer})^{1/2}$. At 235 MHz, the lowest frequency of radio source observations in the present case, the irregularity scale length equals 945 m when the

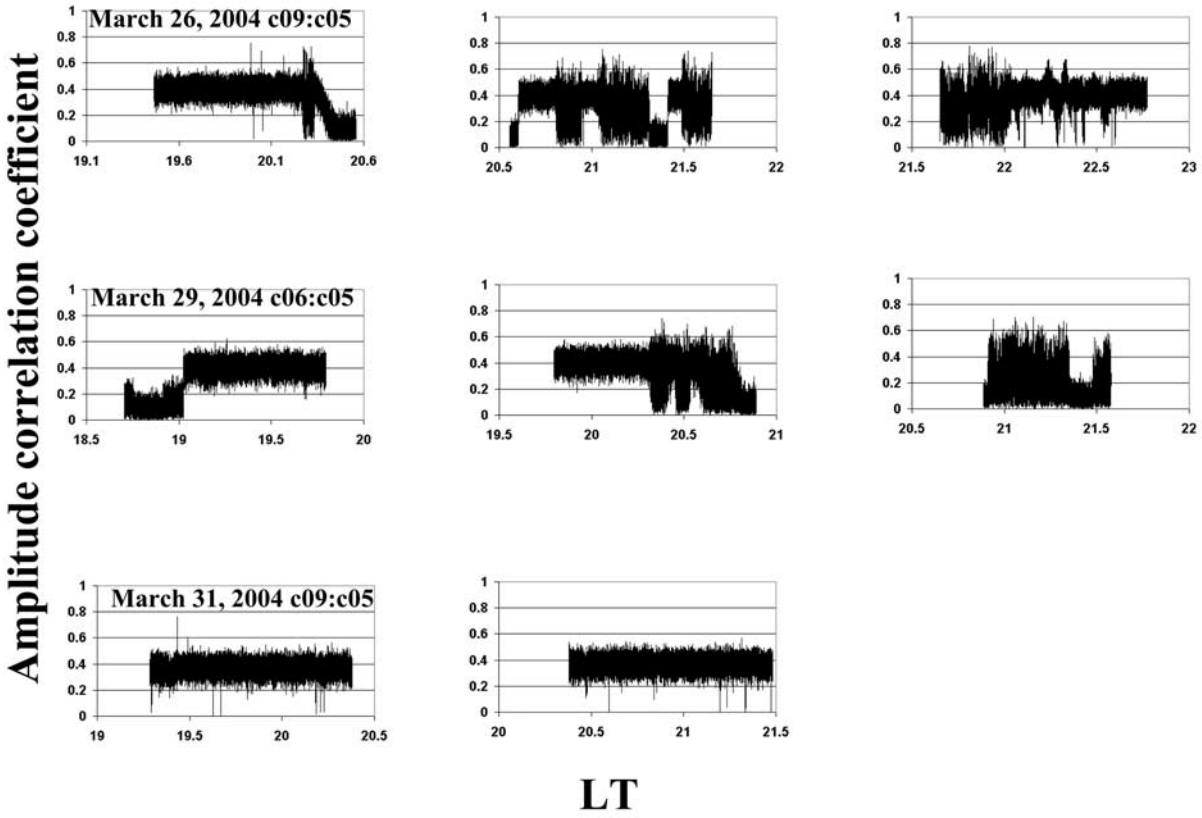


**Figure 3.** Amplitude of signal recorded from radio source 3C218 at GMRT with a sampling interval of 108 ms at 327 MHz during 18.5–22.5 LT on 26, 29, and 31 March 2004, respectively, each arranged in panels of 1.5 h duration from left to right.

irregularity layer height is assumed to be 350 km. The decorrelation of scintillations will occur when the interferometer baseline becomes larger than 945 m. On 26 March 2004, at 235 MHz, the antenna pair C01-C04 was used. Figure 1 shows the baseline for this pair is close to 800 m. Thus decorrelation of scintillations did not occur. At the other extreme frequency of 1420 MHz, the irregularity scale length of 385 m will correspond to the maximum power spectral density. The decorrelation of scintillations at 1420 MHz is expected when the antenna baseline exceeds 385 m. Measurements at 1420 MHz were performed with antenna baselines C12-C10 and C14-C10. These two antenna baselines are of the order of 300 m, which is less than the correlation length of 385 m and the decorrelation of 1420 MHz scintillations did not occur.

[24] A representative plot of the 327 MHz amplitude signal for these three days is shown in Figure 3. On 26 March 2004 scintillation patches could be identified starting from around 20.25 LT and continuing till 22.10 LT after which the original signal level was restored. Four patches of scintillations could be seen occurring during 20.28–20.34 LT, 20.82–20.94 LT, 21.05–21.15 LT, and 21.56–22.04 LT, respectively, with clear breaks in between indicating the drift of discrete patches of irregularities across the radio source-Earth signal propagation path. The signal amplitude dropped to zero level during 20.37–20.60 LT and again during 21.31–21.44 LT as the antenna was pointed away from the source to check antenna pointing. On 29 March 2004, four patches of scintillations could be identified occurring from 20.30–20.44 LT, 20.46–20.58 LT, 20.93–21.37 LT, and finally from 21.49 till the end of the allotted observation period at 21.58 LT. Recording was stopped at 21.58 LT as the allotted observation period was over. On this night also, the signal amplitude dropped to zero during 18.72–19.02 LT, 20.77–20.91 LT, and again from 21.37–21.48 LT as the antenna was pointed away from the source. Actually, only those combinations of antennas were used for which the signal amplitude dropped to zero level with shifted antenna beams. The amplitude record for 31 March 2004

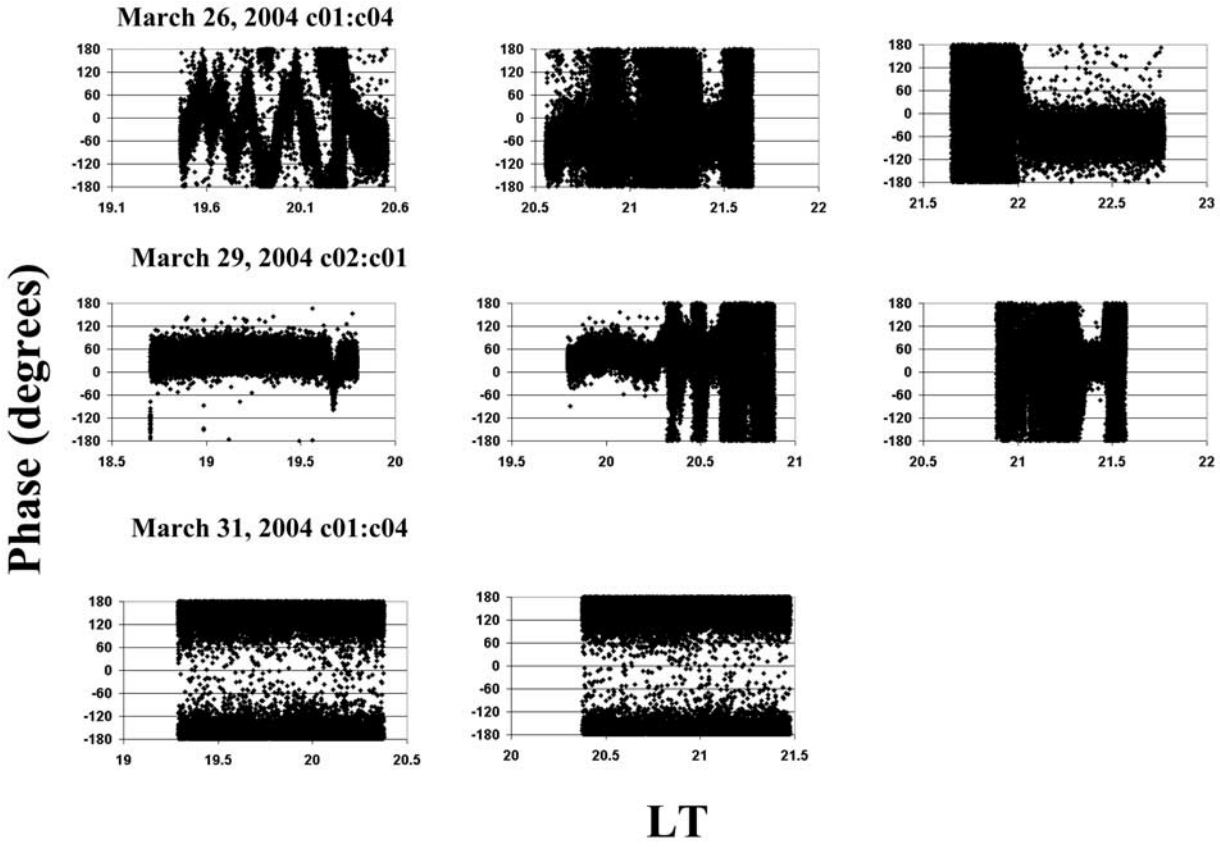


**Figure 4.** Phase of signal recorded from radio source 3C218 at GMRT with a sampling interval of 108 ms at 610 MHz during 18.5–22.5 LT on 26, 29, and 31 March 2004, respectively, each arranged in panels of 1.5 h duration from left to right.

shows no scintillations throughout the period of observation at all the frequencies of operation.

[25] Phase data at 610 MHz recorded on 26, 29, and 31 March 2004 are plotted in Figure 4. Apart from the patches of scintillations, which are observed on the phase records for 26 and 29 March 2004, and also present in the amplitude plots of Figure 3, the most striking feature of this figure is the presence of periodic fluctuations prior to onset of scintillations. On 26 March 2004, oscillatory variations of phase are noted from 19.51–20.17 LT followed by the commencement of scintillations around 20.28 LT. On 29 March 2004, such quasiperiodic fluctuations of phase are observed from 19.84–20.22 LT followed by the occurrences of scintillations from 20.30 LT. The phase records for 31 March 2004 shows concentration of points around ±180° but no periodicity is found at all the other frequencies of observation.

[26] Both the amplitude and the phase data recorded at 108 ms were subject to 16 s moving average to improve the clarity of the figures. Figure 5 shows the moving averaged amplitude data for 26 March 2004 at 235, 327, 610, and 1420 MHz. The moving averaged amplitude data shows the scintillation patches as fadings from the ambient level. Four such fades corresponding to the four patches of scintillations are noted in the amplitude plots at 235, 327, and 610 MHz. However, these fades are not so marked on the 1420 MHz amplitude records, as the intensity of amplitude scintillations decrease with frequency. For a typical three dimensional irregularity spectral index of 4, the magnitude of amplitude scintillations decreases with increasing frequency as $f^{-1.5}$ and the scintillation intensity at 1420 MHz will be a factor of 13 times less than that at 235 MHz.

[27] Figure 6 shows the 16 s moving-averaged phase plots at 235, 327, 610, and 1420 MHz recorded on 26 March 2004. Periodic fluctuations of the signal level are observed at all the frequencies prior to onset of scintillations around 20.25 LT. The amplitudes of oscillations are more at 235 and 327 MHz and gradually become less at 610 and 1420 MHz. The scintillation patches, which

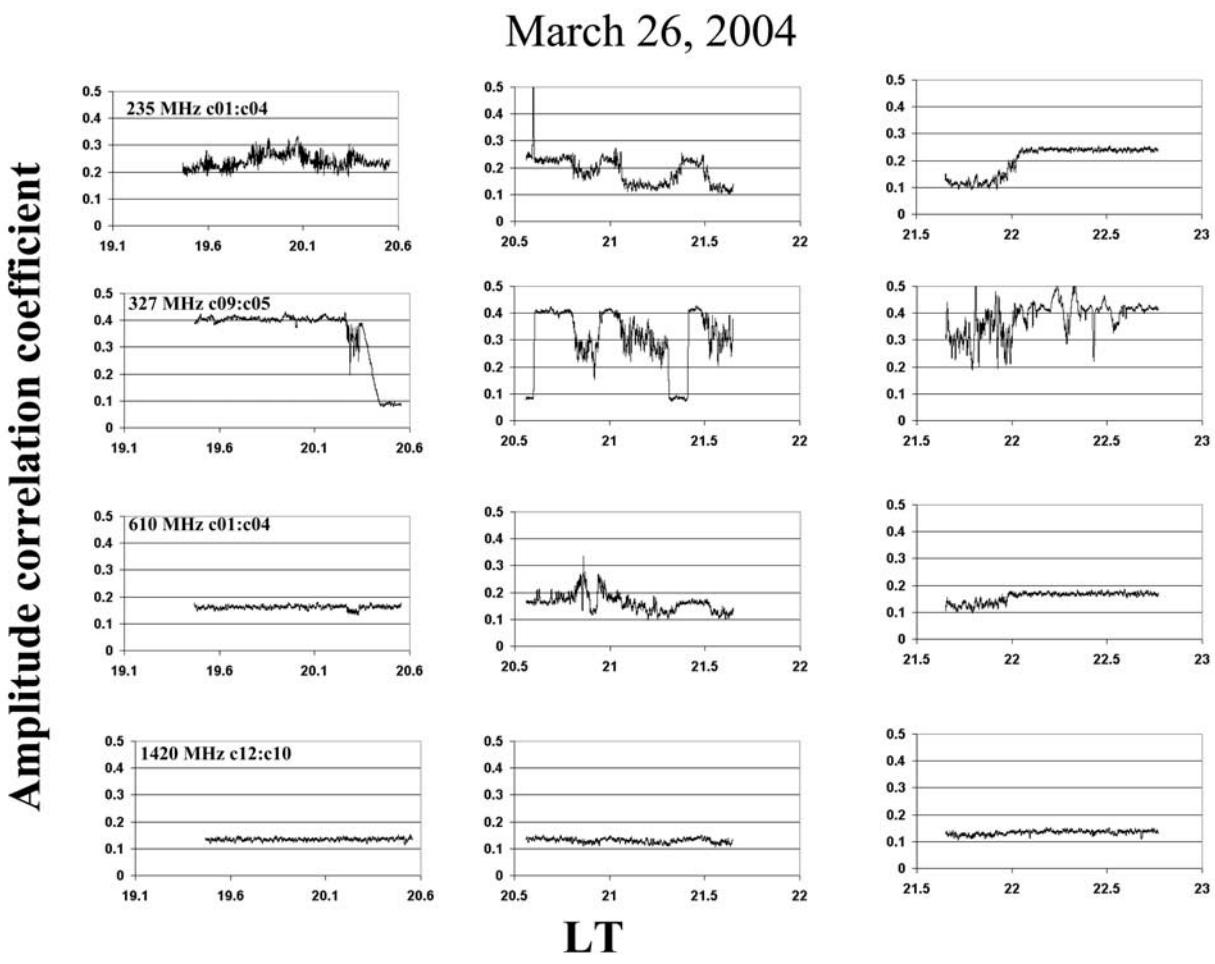


**Figure 5.** The 16 s moving averaged amplitude data recorded at GMRT on 26 March 2004 using signal from the radio source 3C218 recorded at 235, 327, 610, and 1420 MHz, respectively, each arranged in panels of 1.5 h duration from left to right.

continued till 22.10 LT are followed by restoration of signal level, which remained steady till the end of the allotted observation period.

[28] Figure 7 shows the moving averaged amplitude data for 29 March 2004 at 327, 610, and 1420 MHz. Four scintillation patches, which appear as fadings from the ambient level, could be found in the 327 and 610 MHz plots. At the highest frequency of 1420 MHz, the amplitude record, however, does not show any such fading. Periodic nature of variation of phase before the commencement of scintillations are well illustrated in the moving averaged phase plots for 29 March 2004 shown in Figure 8. These precursors of scintillations appear at 327, 610, and 1420 MHz phase records from 19.84–20.22 LT followed by the first scintillation patch around 20.30 LT. On this night, the fourth scintillation patch occurred from 21.49 LT. However, the recording was terminated at 21.58 LT as the allotted time of observation was over.

[29] Figures 9 and 10 show the 16 s moving averaged amplitude and phase plots for 31 March 2004 at 235, 327, 610, and 1420 MHz. No scintillations were observed from GMRT site on that date and the amplitude records do not show any depletion from the ambient level. The phase records on this day show some noise-like fluctuations in contrast to the quasiperiodic structures as seen on 26 and 29 March 2004. On 31 March 2004, the fluctuations occur throughout the period of observations when the amplitude records show no scintillations and are uncorrelated across the frequencies, the 610 MHz channel showing more fluctuations than the 235 and 327 MHz ones.

[30] In order to detect large-scale undulations in the ionization prior to ESF, TEC measured by GPS SV25

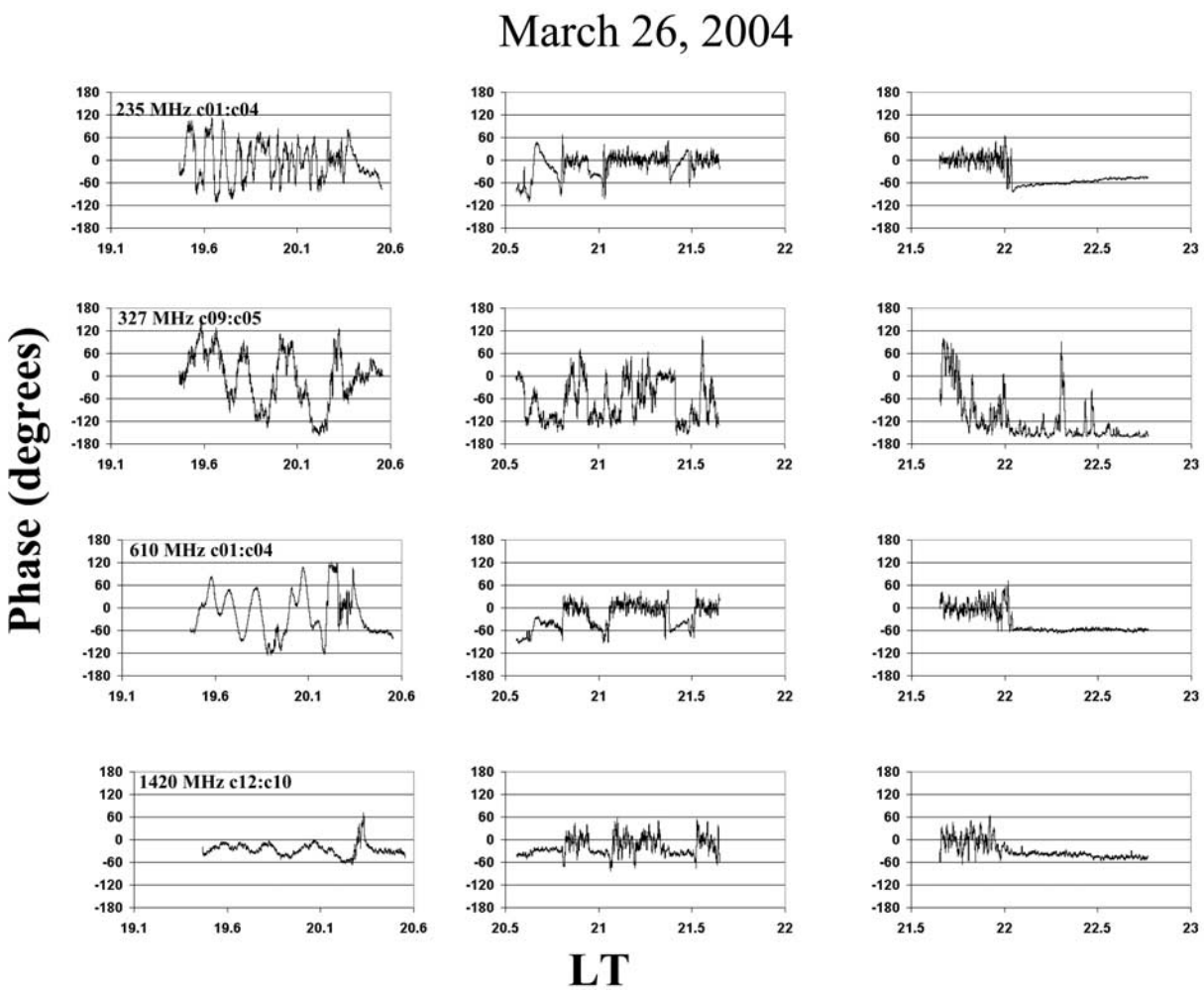


**Figure 6.** The 16 s moving averaged phase data recorded at GMRT on 26 March 2004 using signal from the radio source 3C218 recorded at 235, 327, 610, and 1420 MHz, respectively, each arranged in panels of 1.5 h duration from left to right.

from Mumbai, which is close to GMRT site was studied on 26 March 2004. TEC depletions were noted on this GPS link from 20.85 – 21.25 LT as shown in Figure 11a. The 350 km subionospheric track of SV25 is shown in the Figure 11b. The pierce point of the satellite was around 20°N, 73°E during this time interval. The TEC data was subject to 90-min moving average and the deviations were calculated to eliminate any slow fluctuations. The satellite moved from southwest of the station starting around 17°N, 73°E at 17.50 LT to northeast around 24°N, 77°E at 23 LT. Enlarging the section before the occurrence of depletions and comparing it with the data for 31 March 2004, when no such depletions were noted, prominent periodic fluctuations are observed on 26 March 2004 around 19.50 LT as shown in Figure 11c. It may be noted that periodic fluctuations in TEC with a small amplitude was observed on 31 March 2004 throughout the entire track of SV25. In contrast, the amplitude of the periodic structure is much more prominent on 26 March 2004 before the onset of scintillations and TEC depletions. Another GPS satellite SV15 toward the south of the station also showed periodic structures of amplitude more than 2 TEC units between 18.75 and 20 LT before the onset of the depletion. Signals from GPS SV15, 16, 18, 21, 22, and 25 were recorded for periods varying from 2 to 6 h in the local time interval of interest. In addition to SV15 and 25, SV16, 18, and 22 showed large-scale structures but only toward the edges of the passes at elevations less than 40°. As a result, the

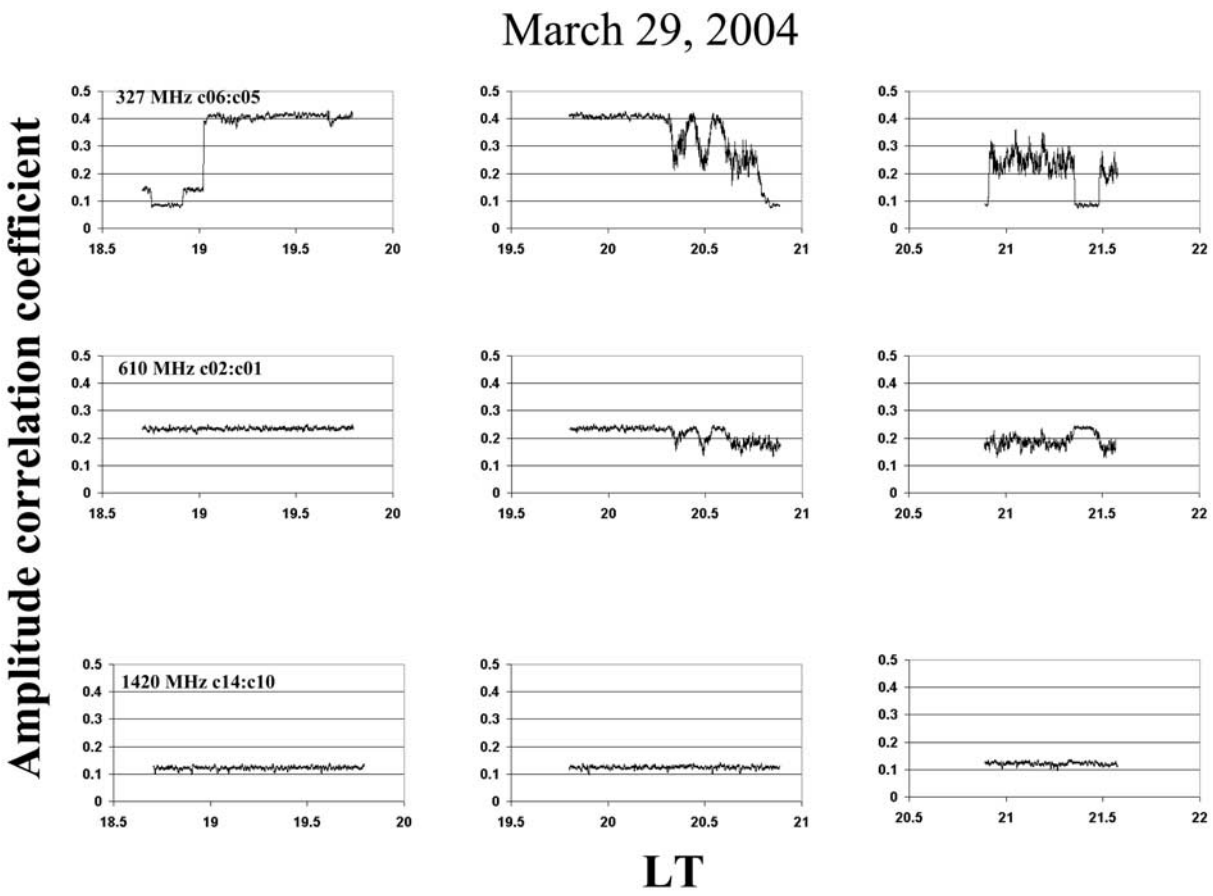


**Figure 7.** The 16 s moving averaged amplitude data recorded at GMRT on 29 March 2004 using signal from the radio source 3C218 recorded at 327, 610, and 1420 MHz, respectively, each arranged in panels of 1.5 h duration from left to right.

deviations from the 90-min moving average could not be estimated.

## 4. Discussions

[31] The present paper reports, for the first time, the results of a multifrequency phase and amplitude measurement of a transionospheric radio signal with a major radio astronomy facility (GMRT) on three days of March 2004. The object of the experiment was to look for possible precursors to generation of ESF using antennas in interferometric mode to receive signals from a radio source located on the southern sky from the station at frequencies ranging from VHF/UHF to L-band.

[32] Extensive research has been carried out for understanding ESF phenomena. Ionosonde, radar backscatter, in situ probe and satellite beacon measurements have developed a general understanding of important ESF processes. Nevertheless, there are a number of outstanding issues underlying ESF formation and evolution that require further attention. The generalized Rayleigh-Taylor instability process has been recognized as the most important destabilizing agent for generation of ESF. However, the question of the source of initial excitation is still open. Background noise is incapable of triggering large-amplitude 100 km wavelength irregularities as reported by many researchers [*Kelley et al.*, 1981; *Tsunoda et al.*, 1982]. *Hysell et al.* [1990] had suggested that gravity waves might be the primary seeding agents for large-scale ESF. They have theoretically related the vertical wavelength of a gravity wave to a plasma layering irregularity that originated at low altitudes and then was convected to higher altitudes. Gravity waves also seem to have determined bottomside intermediate scale undulations. The gravity waves may be generated in the troposphere and then propagate upwards to ionospheric heights. This hypothesis of an external source of large-scale waves in the troposphere is difficult to test.

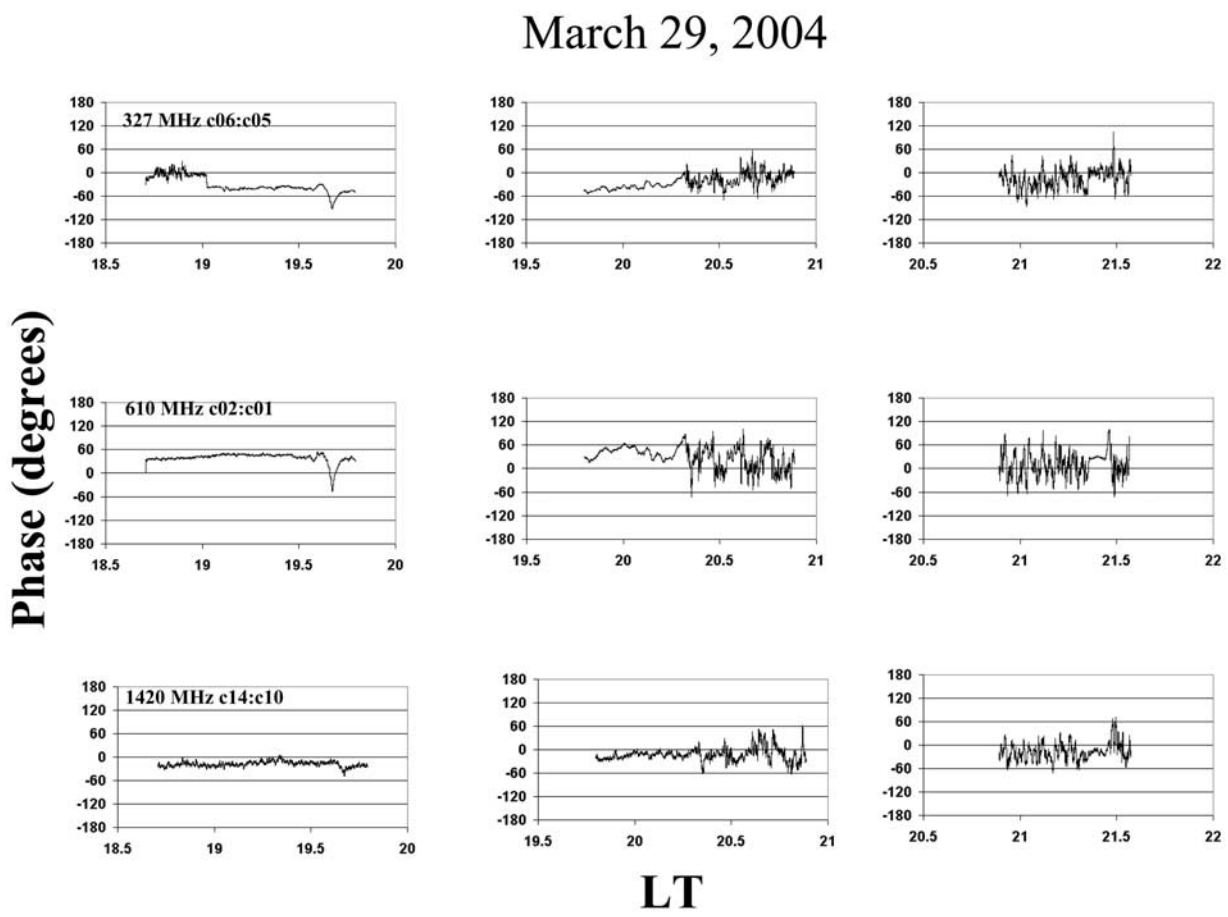


**Figure 8.** The 16 s moving averaged phase data recorded at GMRT on 29 March 2004 using signal from the radio source 3C218 recorded at 327, 610, and 1420 MHz, respectively, each arranged in panels of 1.5 h duration from left to right.

The OH imagers routinely detect gravity wave type of perturbations in the evening at mesospheric heights. However, these waves have not been tracked to the bottomside *F* region. *Hysell et al.* [2006] have established that large-scale seed waves that drive the Rayleigh-Taylor instability to cause spread *F* are generated within the ionosphere system. These have been detected in the bottomside equatorial *F* region and are generated by the collisional shear instabilities during the postsunset hours. The wave structures may propagate obliquely through the base of the ionosphere to the topside and may have significant horizontal velocity component [*Vadas and Fritts*, 2006; *Vadas*, 2007]. However, the role of the gravity waves is believed to be merely to initiate ESF activity rather than sustaining it. Alternatively, *Tsunoda* [2007] have suggested that a polarization electric field, if generated by sporadic *E* layer instability should map to the base of the *F* layer and seed equatorial plasma bubbles.

[33] The large-scale periodic structures may be taken as precursors to onset of ESF. Although the ESF irregularities may have localized generation, the bubble has an explosive development through nonlinear Rayleigh-Taylor instability, extending over a few hundred kilometers in the east-west as well as topside direction. An entire field tube takes part in the irregularity generation mechanism and is upwelled to the topside in the form of a 'peeled orange section' [*Haerendel*, 1974]. The motion of the bubble has been discussed by *Anderson and Haerendel* [1979]. Radar backscatter maps at Pohnpei Island (7.0°N, 158.2°E geographic; 0.4°N dip latitude) and Tirupati (13.5°N, 79.2°E geographic; 6.3°N dip latitude), India show large-scale undulations, which may extend about 200 km in altitude [*Rao et al.*, 1997; *Tsunoda and Ecklund*, 2007]. Simultaneous records of scintillations from Delhi near the northern crest of the equatorial ionization anomaly and Madras, close to the magnetic equator show that the occurrence of scintillations

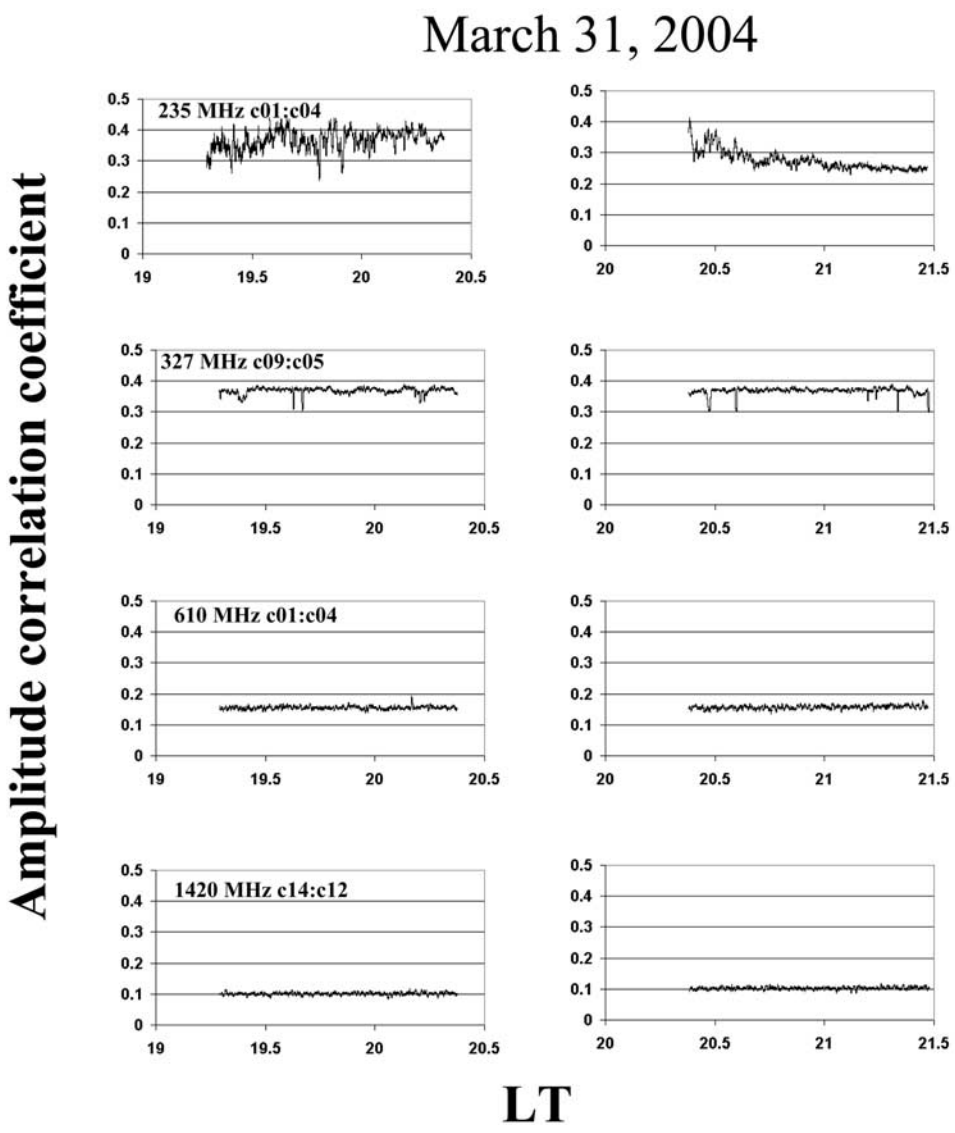


**Figure 9.** The 16 s moving averaged amplitude data recorded at GMRT on 31 March 2004 using signal from the radio source 3C218 recorded at 235, 327, 610, and 1420 MHz, respectively, each arranged in panels of 1.5 h duration from left to right.

at Delhi is conditional to their prior occurrence at Madras with the field line apex heights over the magnetic equator being 1200 and 400 km, respectively [*Dabas et al.*, 1998].

[34] Smaller scale irregularities covering scale sizes over six decades from millimeter to kilometer size are generated at the walls of the bubble [*Kelley*, 1989]. The correspondence between the large-scale wave-like precursors and the irregularities generated within the bubble is yet to be established. Amplitude scintillations is effectively produced by irregularities of the dimension of the first Fresnel zone while the phase fluctuations are controlled by irregularities over extended scale sizes.

[35] The major objective behind conducting the experiment at GMRT was to examine from the phase data if any large scale periodic undulations are present prior to onset of scintillations, and based on that to establish whether an alert could be issued for possible use by radio astronomers and other transionospheric link users. The phase of a transionospheric signal is directly proportional to the TEC in the path from the source to the antenna. In interferometric measurements, when there is no perturbation in the ionosphere, the recorded phase normally corresponds to a steady path difference between the two rays at the antennas. Any time-dependent perturbation

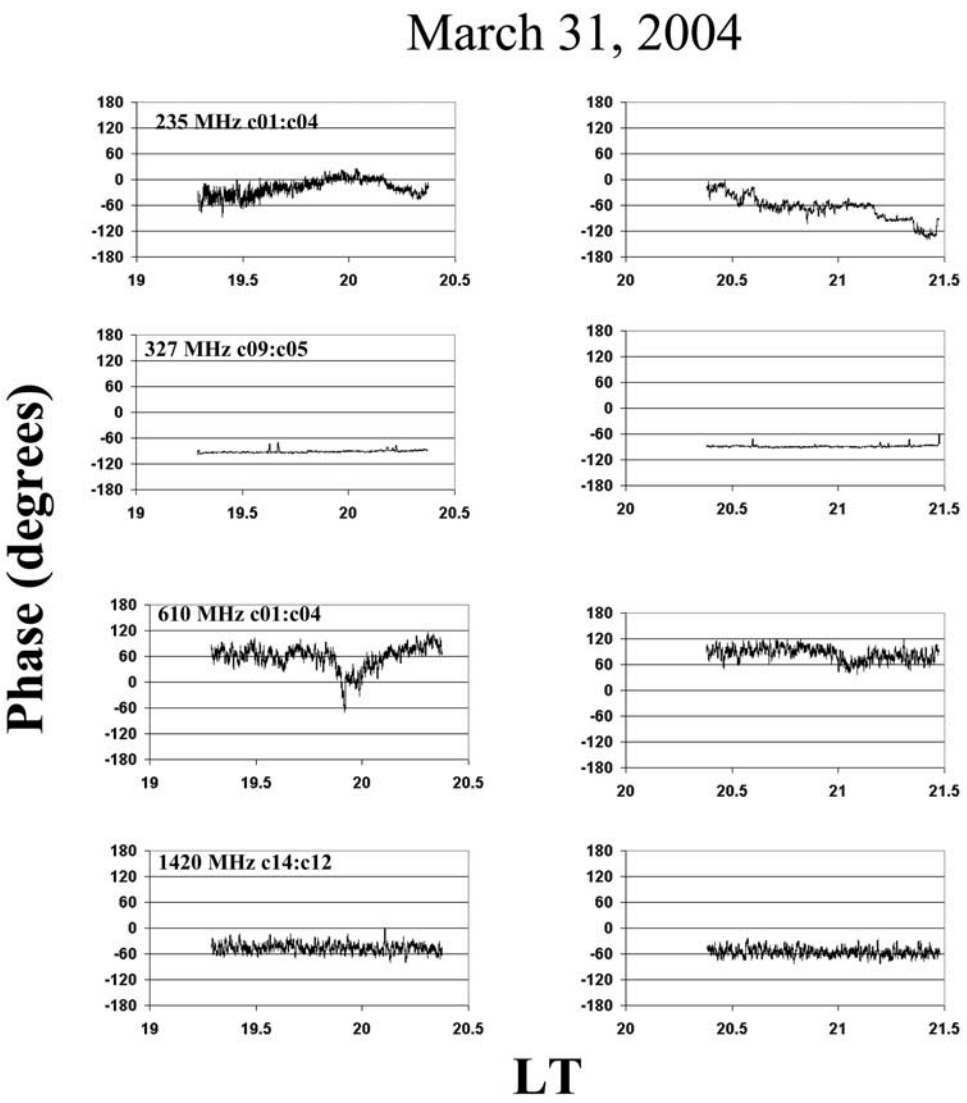


**Figure 10.** The 16 s moving averaged phase data recorded at GMRT on 31 March 2004 using signal from the radio source 3C218 recorded at 235, 327, 610, and 1420 MHz, respectively, each arranged in panels of 1.5 h duration from left to right.

propagating in the medium will produce a corresponding deviation of the recorded phase. The periodic structures observed in the phase of a transionospheric radio signal may undulate the bottomside of the ionosphere as observed with radars by *Tsunoda and White* [1981], *Tsunoda et al.* [1982], *Hysell et al.* [1990], and *Tsunoda and Ecklund* [2007]. TEC, which gives the integrated electron density up to the satellite is very much weighted by the electron density slab around the height of maximum ionization ($h_mF_2$). Any periodic signature in TEC implies propagation of the periodic perturbations up to at least the height of maximum ionization. In other words, for generation of ESF, the undulating large-scale ionospheric perturbations should propagate to the height of maximum ionization and beyond. GPS SV25 from Mumbai measured large amplitude TEC oscillations of period 34 mins on 26 March 2004 under the GAGAN program.

[36] The 350 km subionospheric track of the radio source 3C218 is situated in the southern sky of GMRT during the period of observation. As the location of GMRT is between the magnetic equator and the northern crest of the equatorial anomaly in the Indian longitude sector, irregularities developing over the magnetic equator in the early evening hours will move across the radio propagation path connecting the source and the ground-

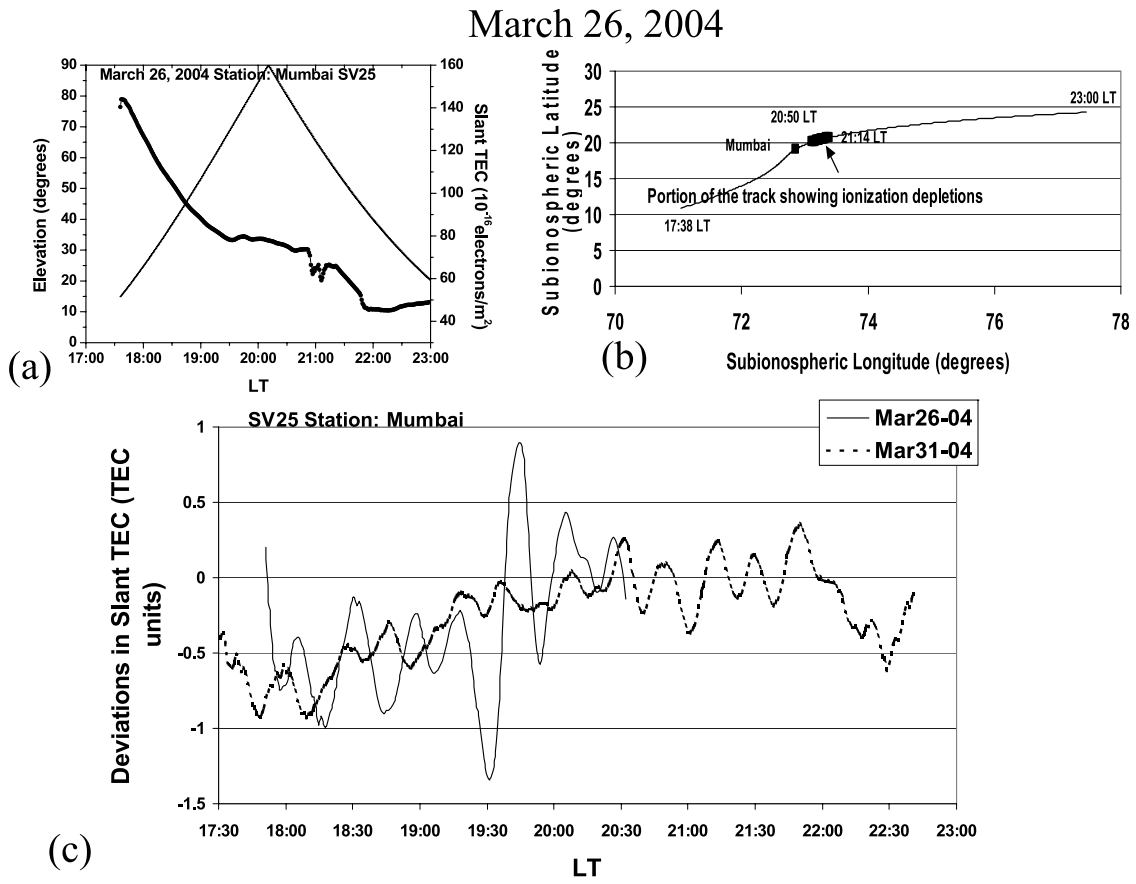


**Figure 11.** (a) Plot of Slant TEC and elevation measured using GPS SV25 on 26 March 2004 from station Mumbai. (b) The 350 km subionospheric track of GPS SV25 from Mumbai. Location of Mumbai and portion of the track showing TEC depletions are indicated. (c) Comparative plot of deviations of Slant TEC from 90-min moving average measured using GPS SV25 on 26 and 31 March 2004 from Mumbai.

based receiver. The 350 km subionospheric point of the radio source maps up to 500 km over the magnetic equator. Electric field perturbations associated with the large-scale periodic structures over the magnetic equator may be coupled to off-equatorial ionospheric locations and vice versa along the highly conducting geomagnetic field lines. Observations were confined to the time interval 18.5–22.5 LT on all the days, namely, 26, 29, and 31 March 2004. Patches of scintillations were identified in the amplitude and phase plots on all days except 31 March 2004. The striking feature of the plots was the presence of periodic structures in the phase data prior to onset of scintillations on 26 and 29 March 2004 at the different frequencies. The possible precursors of ESF noted on the phase plots occurred about 50 min before the onset of scintillations. This advance warning time margin was almost same at all the operating frequencies of GMRT i.e., 235, 327, 610, and 1420 MHz on days of ESF occurrence, namely, 26 and 29 March 2004. The amplitude of the periodic fluctuations had an inverse dependence on the operating frequency.

[37] A very important component of the International Space Weather campaign is associated with prediction of scintillations. Several techniques for forecasting postsunset equatorial scintillations have been suggested and their merits and demerits discussed by *Ray et al.* [2006]. The simplest and least expensive of these methods involve measurement of latitudinal gradient of TEC in the region between the trough and the crest of the equatorial ionization anomaly during the local afternoon hours of equinoctial months of high sunspot number years using transmissions from low Earth orbiting satellites. Prediction of scintillations based on periodic fluctuations of the phase of an interferometric signal at GMRT prior to onset of scintillations has the advantage that the predictive

mechanism is built-in within the measuring system and does not require any separate installation.

[38] Identification of precursors in the phase records provides a very important and useful tool for issuing an alerting service for possible use by radio astronomers and other transionospheric link users, particularly in the equatorial and low-latitudes radio astronomical facilities where occurrence of ESF during the equinoxes of high sunspot number years is very intense and frequent. Prior forecasting of equatorial scintillations would be very useful for satellite-based communication and navigation system user community as the performance of these systems is severely compromised during periods of intense ESF.

[39] **Acknowledgments.** The authors are grateful to the late A. P. Mitra and Santimay Basu and Sunanda Basu for encouragement in undertaking the experiment and discussions. The cooperation of R. Nityananda and other staff at GMRT is thankfully acknowledged. The GAGAN data were obtained from Space Application Center, Ahmedabad, India, through K. K. Bandyopadhyay and M. R. Sivaraman. Ionosonde data from Trivandrum were kindly provided by R. Sridharan and Sudha Ravindran. A part of this research has been sponsored by the Indian Space Research Organization (ISRO) through projects at the S. K. Mitra Center for Research in Space Environment, University of Calcutta. The authors thank the referees for critical reading of the manuscript and suggestions for improvement.

## References

Anderson, D. N., and G. Haerendel (1979), The motion of depleted plasma regions in the equatorial ionosphere, *J. Geophys. Res.*, *84*(A8), 4251–4256.

Basu, S., and S. Basu (1976), Correlated measurements of scintillations and in situ *F* region irregularities from OGO-6, *Geophys. Res. Lett.*, *3*, 681–684.

Basu, S., and H. E. Whitney (1983), The temporal structure of intensity scintillations near the magnetic equator, *Radio Sci.*, *18*(2), 263–271.

Bhar, J. N., A. DasGupta, and S. Basu (1970), Studies on *F* region irregularities at low latitude from scintillation of satellite signals, *Radio Sci.*, *5*, 939–942.

Dabas, R. S., D. R. Lakshmi, and B. M. Reddy (1998), Day-to-day variability in the occurrence of equatorial and low-latitude scintillations in the Indian zone, *Radio Sci.*, *33*(1), 89–96.

DasGupta, A., and L. Kersley (1976), Summer daytime scintillation and sporadic *E*, *J. Atmos. Terr. Phys.*, *38*, 615–618.

DasGupta, A., A. Paul, S. Ray, A. Das, and S. Ananthakrishnan (2006), Equatorial bubbles as observed with GPS measurements over Pune, India, *Radio Sci.*, *41*, RS5S28, doi:10.1029/2005RS003359.

Fejer, B. G., and M. C. Kelley (1980), Ionospheric irregularities, *Rev. Geophys.*, *18*, 401–454.

Guzdar, P. N., P. Satyanarayana, J. D. Huba, and S. L. Ossakow (1982), Influence of velocity shear on Rayleigh-Taylor instability, *Geophys. Res. Lett.*, *9*, 547–550.

Haerendel, G. (1974), Theory of equatorial spread *F*, report, Max Planck-Inst. für Phys. Und Astrophys., Garching, Germany.

Hanson, W. B., and S. Sanatani (1973), Large $N_I$ gradients below the equatorial *F* peak, *J. Geophys. Res.*, *78*, 1167–1173.

Hassam, A. B. (1992), Nonlinear stabilization of the Rayleigh-Taylor instability by external velocity shear, *Phys. Fluids*, *4*, 485–487.

Huba, J. D., and L. C. Lee (1983), Short wavelength stabilization of the gradient drift instability due to velocity shear, *Geophys. Res. Lett.*, *10*, 357–360.

Hysell, D. L., and E. Kudeki (2004), Collisional shear instability in the equatorial *F* region ionosphere, *J. Geophys. Res.*, *109*, A11301, doi:10.1029/2004JA010636.

Hysell, D. L., M. C. Kelley, W. E. Swartz, and R. F. Woodman (1990), Seeding and layering of equatorial spread *F* by gravity waves, *J. Geophys. Res.*, *95*, 17,253–17,260.

Hysell, D. L., M. F. Larsen, C. M. Swenson, and T. F. Wheeler (2006), Shear flow effects at the onset of equatorial spread *F*, *J. Geophys. Res.*, *111*, A11317, doi:10.1029/2006JA011963.

Kelley, M. C. (1989), *The Earth's Ionosphere: Plasma Physics and Electrodynamics*, Academic, San Diego, Calif.

Kelley, M. C., G. Haerendal, H. Kappler, A. Valenzuela, B. B. Balsley, D. A. Carter, W. L. Ecklund, C. W. Carlson, B. Hausler, and R. Torbert (1976), Evidence for a Rayleigh-Taylor type instability and upwelling of depleted density regions during equatorial spread *F*, *Geophys. Res. Lett.*, *3*, 448–450.

Kelley, M. C., M. F. Larsen, C. LaHoz, and J. P. McClure (1981), Gravity wave initiation of equatorial spread *F*, *J. Geophys. Res.*, *86*, 9087–9100.

Kelley, M. C., et al. (1986), The Condor equatorial spread F campaign: Overview of results of the large-scale measurements, *J. Geophys. Res.*, *91*, 5487–5503.

Kil, H., and R. A. Heelis (1998a), Global distribution of density irregularities in the equatorial ionosphere, *J. Geophys. Res.*, *103*, 407–417.

Kintner, P. M., B. M. Ledvina, E. R. de Paula, and I. J. Kantor (2004), Size, shape, orientation, speed, and duration of GPS equatorial anomaly scintillations, *Radio Sci.*, *39*, RS2012, doi:10.1029/2003RS002878.

Klostermeyer, J. (1978), Nonlinear investigation of the spatial resonance effect in the nighttime equatorial *F* region, *J. Geophys. Res.*, *83*, 3753–3760.

Kudeki, E., B. G. Fejer, D. T. Farley, and H. M. Ierkic (1981), Interferometer studies of equatorial *F* region irregularities and drifts, *Geophys. Res. Lett.*, *8*, 377–388.

McClure, J. P., W. B. Hanson, and J. H. Hoffman (1977), Plasma bubbles and irregularities in the equatorial ionosphere, *J. Geophys. Res.*, *82*, 2650–2656.

Rao, P. B., A. K. Patra, T. V. Chandrasekhar Sarma, B. V. Krishna Murthy, K. S. V. Subba Rao, and S. S. Hari (1997), Radar observations of updrafting and downdrafting plasma depletions associated with the equatorial spread *F*, *Radio Sci.*, *32*(3), 1215–1227.

Ray, S., A. Paul, and A. DasGupta (2006), Equatorial scintillations in relation to the development of ionization anomaly, *Ann. Geophys.*, *24*, 1429–1442.

Rishbeth, H. (1971), Polarization fields produced by winds in the equatorial *F* region, *Planet. Space Sci.*, *19*, 357–369.

Rottger, J. (1973), Wavelike structures of large scale equatorial spread *F* irregularities, *J. Atmos. Terr. Phys.*, *35*, 1195–1196.

Rottger, J. (1976), The macro-scale structure of equatorial spread *F* irregularities, *J. Atmos. Terr. Phys.*, *38*, 97–101.

Rottger, J. (1978), Drifting patches of equatorial spread *F* irregularities–Experimental support for the spatial resonance mechanism in the ionosphere, *J. Atmos. Terr. Phys.*, *40*, 1103–1112.

Rufenach, C. L. (1972), Power-law wavenumber spectrum deduced from ionospheric scintillation observations, *J. Geophys. Res.*, *77*, 4761–4772.

Rufenach, C. L. (1975), Ionospheric scintillation by a random phase screen: Spectral approach, *Radio Sci.*, *10*(2), 155–165.

Sekar, R., and M. C. Kelley (1998), On the combined effects of vertical shear and zonal electric field patterns on nonlinear equatorial spread *F* evolution, *J. Geophys. Res.*, *103*, 20,735–20,748.

Swarup, G., S. Ananthakrishnan, V. K. Kapahi, A. P. Rao, C. R. Subramanya, and V. K. Kulkarni (1991), The Giant Meterwave Radio Telescope, *Curr. Sci.*, *60*(2), 95–105.

Tsunoda, R. T. (2007), Seeding of equatorial plasma bubbles with electric fields from an $E_s$-layer instability, *J. Geophys. Res.*, *112*, A06304, doi:10.1029/2006JA012103.

Tsunoda, R. T., and W. L. Ecklund (2007), On the post-sunset rise of the equatorial *F* layer and superposed upwellings and bubbles, *Geophys. Res. Lett.*, *34*, L04101, doi:10.1029/2006GL028832.

Tsunoda, R. T., and B. R. White (1981), On the generation and growth of equatorial backscatter plumes: 1. Wave structure in the bottomside *F* layer, *J. Geophys. Res.*, *86*, 3610–3616.

Tsunoda, R. T., R. C. Livingston, and C. L. Rino (1981), Evidence of a velocity shear in bulk plasma motion associated with the post-sunset rise of the equatorial *F* layer, *Geophys. Res. Lett.*, *8*, 807–810.

Tsunoda, R. T., R. C. Livingston, J. P. McClure, and W. B. Hanson (1982), Equatorial plasma bubbles: Vertically elongated wedges from the bottomside *F* layer, *J. Geophys. Res.*, *87*(A11), 9171–9180.

Vadas, S. L. (2007), Horizontal and vertical propagation and dissipation of gravity waves in the thermosphere from lower atmosphere and thermosphere sources, *J. Geophys. Res.*, *112*, A06305, doi:10.1029/2006JA011845.

Vadas, S. L., and D. C. Fritts (2006), Influence of solar variability on gravity wave structure and dissipation in the thermosphere from tropospheric convection, *J. Geophys. Res.*, *111*, A10S12, doi:10.1029/2005JA011510.

Weber, E. J., J. Buchau, and J. G. Moore (1980), Airborne studies of equatorial *F* layer ionospheric irregularities, *J. Geophys. Res.*, *85*, 4621–4641.

Woodman, R. F., and C. La Hoz (1976), Radar observations of *F* region equatorial irregularities, *J. Geophys. Res.*, *81*, 5447–5466.

S. Ananthakrishnan, Department of Electronic Science, University of Pune, 411007 Pune, India.

A. Das, A. DasGupta, and S. Ray, S. K. Mitra Center for Research in Space Environment, University of Calcutta, 700009 Calcutta, India. (adg1bkpr@hotmail.com)

A. Paul, Institute of Radio Physics and Electronics, University of Calcutta, 700009 Calcutta, India.